

Maize *opaque5* Encodes Monogalactosyldiacylglycerol Synthase and Specifically Affects Galactolipids Necessary for Amyloplast and Chloroplast Function

Alan M. Myers,^{a,1} Martha G. James,^{a,1} Qiaohui Lin,^a Gibum Yi,^b Philip S. Stinard,^c Tracie A. Hennen-Bierwagen,^a and Philip W. Becraft^{b,2}

^aDepartment of Biochemistry, Biophysics, and Molecular Biology, Iowa State University, Ames, Iowa 50011

^bDepartment of Genetics, Development, and Cell Biology, Iowa State University, Ames, Iowa 50011

^cU.S. Department of Agriculture/Agricultural Research Service, Maize Genetics Cooperation Stock Center, Urbana, Illinois 61801

The maize (*Zea mays*) *opaque5* (*o5*) locus was shown to encode the monogalactosyldiacylglycerol synthase MGD1. Null and point mutations of *o5* that affect the vitreous nature of mature endosperm engendered an allelic series of lines with stepwise reductions in gene function. C_{18:3}/C_{18:2} galactolipid abundance in seedling leaves was reduced proportionally, without significant effects on total galactolipid content. This alteration in polar lipid composition disrupted the organization of thylakoid membranes into granal stacks. Total galactolipid abundance in endosperm was strongly reduced in *o5*⁻ mutants, causing developmental defects and changes in starch production such that the normal simple granules were replaced with compound granules separated by amyloplast membrane. Complete loss of MGD1 function in a null mutant caused kernel lethality owing to failure in both endosperm and embryo development. The data demonstrate that low-abundance galactolipids with five double bonds serve functions in plastid membranes that are not replaced by the predominant species with six double bonds. Furthermore, the data identify a function of amyloplast membranes in the development of starch granules. Finally, the specific changes in lipid composition suggest that MGD1 can distinguish the constituency of acyl groups on its diacylglycerol substrate based upon the degree of desaturation.

INTRODUCTION

Maize (*Zea mays*) mutations that cause opaque kernel phenotypes are of interest because of their effects on seed texture and nutritional quality traits. The phenotype is defined by kernels that appear opaque to transmitted light, as opposed to the partially translucent appearance of normal vitreous seeds. At least 18 *opaque* gene loci are known, some of which are involved in storage protein metabolism (Thompson and Larkins, 1994; Hunter et al., 2002). The *opaque2* (*o2*) locus, for example, encodes a transcription factor that activates genes coding for α -zein proteins, thus changing the constituency of protein bodies made in the endoplasmic reticulum (ER) and present in mature endosperm after desiccation (Kodrzycki et al., 1989; Schmidt et al., 1990). Another example is *floury1*, which encodes a membrane protein involved in targeting an α -zein to the interior of protein bodies (Holding et al., 2007). Macromolecular assembly

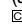
of protein bodies is highly complex (Holding and Larkins, 2009), possibly explaining why *opaque* loci are identified frequently. In many instances, however, the cause of the phenotype appears to be unrelated to protein composition. For example, altered starch composition conferred by *waxy1* mutations causes kernel opacity (reviewed in Coe et al., 1988). Similarly, mutations of the *o5* locus condition opaque kernels without notable changes in total protein content, zein versus nonzein ratio, or amino acid composition (Hunter et al., 2002).

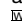
In this study, *o5* was found to code for a glycosyl transferase that generates monogalactosyldiacylglycerol (MGDG). MGDG and digalactosyldiacylglycerol (DGDG) are the primary nonprotein components of plastid membranes, providing both structural and functional organization. Together, these galactolipids account for as much as 80% of total polar lipid content in plastids (Block et al., 1983; Dörmann and Benning, 2002; Hölzl and Dörmann, 2007). Galactolipid-based membranes are conserved features of organisms that undergo oxygenic photosynthesis, including Chloroplastida and cyanobacteria. Direct functions in photosynthesis are possible because specific galactolipids appear as ligands in three dimensional structures of photosynthetic complexes (Jordan et al., 2001; Loll et al., 2007). In addition, owing to its nonbilayer forming properties, MGDG is likely to provide membrane structure in areas of tight turns and high protein packing density (Webb and Green, 1991; Bruce, 1998; Lee, 2000; Dörmann and Benning, 2002). Nonphotosynthetic plastid membranes also contain MGDG and DGDG in high abundance, so

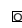
¹These authors contributed equally to this work.

²Address correspondence to becraft@iastate.edu.

The authors responsible for distribution of materials integral to the findings presented in this article in accordance with the policy described in the Instructions for Authors (www.plantcell.org) are: Alan M. Myers (ammyers@iastate.edu) and Philip W. Becraft (becraft@iastate.edu).

Some figures in this article are displayed in color online but in black and white in the print edition.

Online version contains Web-only data.

Open Access articles can be viewed online without a subscription. www.plantcell.org/cgi/doi/10.1105/tpc.111.087205

galactolipid function is not restricted to light harvesting or electron transfer. Most higher-plant MGDG has a C₁₈/C₁₈ molecular structure, with an 18:3 fatty acid at both the *sn*-1 and *sn*-2 positions of the glycerol backbone. Some plants also contain MGDG with C₁₈/C₁₆ structures (Heinz, 1977; Maréchal et al., 2000). The C₁₈/C₁₈ species are thought to be derived from the ER lipid assembly pathway using fatty acids exported from the plastid, whereas C₁₈/C₁₆ lipids arise from the organellar lipid assembly pathway (Benning, 2008).

The enzyme MGDG synthase (MGD) (UDPGalactose: 1,2-diacylglycerol 3-β-D-galactosyl-transferase; EC 2.4.1.46), located in plastid envelope membranes, catalyzes transfer of a galactosyl residue from UDPgalactose to the *sn*-3 position of diacylglycerol (DAG) (Dörmann and Benning, 2002; Benning and Ohta, 2005). MGD activity has been studied most extensively in *Arabidopsis thaliana*, spinach (*Spinacia oleracea*), and cucumber (*Cucumis sativus*) (Joyard and Douce, 1987; Shimojima et al., 1997; Maréchal et al., 2000). MGD enzymes in these plants are divided into type A and type B classes based on amino acid sequences as well as enzymatic and physiological properties. The type A enzyme (MGD1) is targeted to the inner plastid envelope membrane, whereas the two type B enzymes (MGD2 and MGD3) are localized to outer envelope membranes (Maréchal et al., 2000; Awai et al., 2001). MGD1 is expressed in all plant tissues and is the most abundant form in chloroplasts, whereas MGD2 and MGD3 are detected primarily in nonphotosynthetic tissues, including flowers and roots (Awai et al., 2001; Kobayashi et al., 2004). MGD2 and MGD3 are induced by phosphate starvation, suggesting they function in specific conditions, whereas MGD1 appears to serve a general role in galactolipid biosynthesis based on its constitutive expression pattern (Awai et al., 2001; Kobayashi et al., 2004).

In *Arabidopsis*, the hypomorphic point mutation *mgd1-1* conditioned chlorotic plants that exhibit ~50% reduction in chlorophyll (Jarvis et al., 2000). MGDG content was reduced to ~42% of normal, although total leaf lipid content was similar to the wild type. Chloroplasts were underdeveloped in the mutant, with reduced numbers of starch granules. The null allele *mgd1-2* conditioned a near absence of both MGDG and DGDG as well as disruption of the photosynthetic plastid membranes, leading to a loss of photosynthetic ability for the plant (Kobayashi et al., 2007). Embryo development also was impaired in *mgd1-2* mutants and the seeds were white, indicating that galactolipids have an essential role in embryogenesis (Kobayashi et al., 2007). These results indicate that neither MGD2 nor MGD3 compensates for loss of MGD1 in *Arabidopsis*.

This study characterized the effects of reducing or eliminating MGD1 function in leaves and endosperm of maize, a C4 monocot. The finding that mutations affecting MGD1 cause an opaque endosperm phenotype reveals a connection between membrane structure and storage compound metabolism in nonphotosynthetic plastids. Additionally, a hypomorphic *o5*⁻ allele specifically affects abundance of minor MGDG or DGDG species with five double bonds in the two acyl groups combined. This seemingly subtle change in lipid structure, with essentially no reduction in the total galactolipid content, is physiologically significant. The data further reveal that acyl group identity can be a factor for MDG1 enzyme activity. In an *o5* null mutant, as was observed in

Arabidopsis, maize embryo development is aborted at an early stage, indicating that galactolipid function is essential in non-photosynthetic and photosynthetic tissue.

RESULTS

Multiple Alleles of the *o5* Locus and Resultant Phenotypes

The mutation *o5-Ref*, which causes visually distinctive opaque kernel and pale green virescent seedling phenotypes (Figures 1A and 1B), was first described by Robertson in 1967 (www.maizegdb.org). Other mutations that cause opaque kernels were subjected to complementation tests by crossing heterozygous mutants to homozygous *o5-Ref* plants. In three instances, ~50% of the progeny kernels were opaque, thus identifying new *o5*⁻ alleles. These mutations, termed *o5-PS3038*, *o5-5288*, and *o5-313328*, condition various kernel and seedling phenotypes (summarized in Supplemental Table 1 online).

Both *o5-Ref* and *o5-313328* condition pale-green, virescent seedlings that subsequently acquire full green color and develop apparently normally through maturity. Homozygous kernels bearing either mutation are opaque and slightly pale compared with yellow kernels of the congenic wild-type inbred W64A but germinate normally and exhibit near-normal morphology. The *o5-5288* allele causes a stronger phenotype with white seedlings that fail to acquire green color and die 7 to 14 d postemergence. The kernel morphology of *o5-5288* homozygotes is white and shrunken. The mutation *o5-PS3038* is the most severe in this allelic group because it conditions defective kernels that fail to germinate. Mutant kernels observed on a segregating ear from a self-pollinated *o5-PS3038/+* heterozygote are white and frequently severely shrunken (Figure 1C). The latter two mutations must be maintained as heterozygotes because homozygous individuals are nonviable.

Another allelic combination examined in this study is the *o5-Ref/o5-PS3038* compound heterozygote. Such kernels are lighter in color and slightly collapsed at the crown compared with homozygous *o5-Ref* kernels. Seedlings grown from these kernels remain chlorotic and die within 2 weeks of emergence (Figure 1B), similar to *o5-5288* homozygotes.

Molecular Characterization of the *o5* Locus

Transposon tagging was used to identify the *o5* locus. As described previously, a *Mu8* transposable element insertion was found tightly linked to the *o5* locus (Yi et al., 2009). Briefly, an *o5-PS3038/+* heterozygote was crossed to an *o5-Ref* homozygote to generate a population segregating 1:1 for *o5-PS3038/o5-Ref* mutant and *+/o5-Ref* normal offspring. As expected, approximately one-half of the kernels on such ears displayed the opaque phenotype. DNA isolated from mutant and normal seedlings was subjected to a high-throughput transposon display method called MuTA. A unique amplification product containing a *Mu8* terminus and flanking genomic DNA was identified in all four *o5-PS3038/o5-Ref* mutant DNA samples and was absent in all four *+/o5-Ref* normal samples. The sequence of this product matched exactly to a published EST (GenBank accession

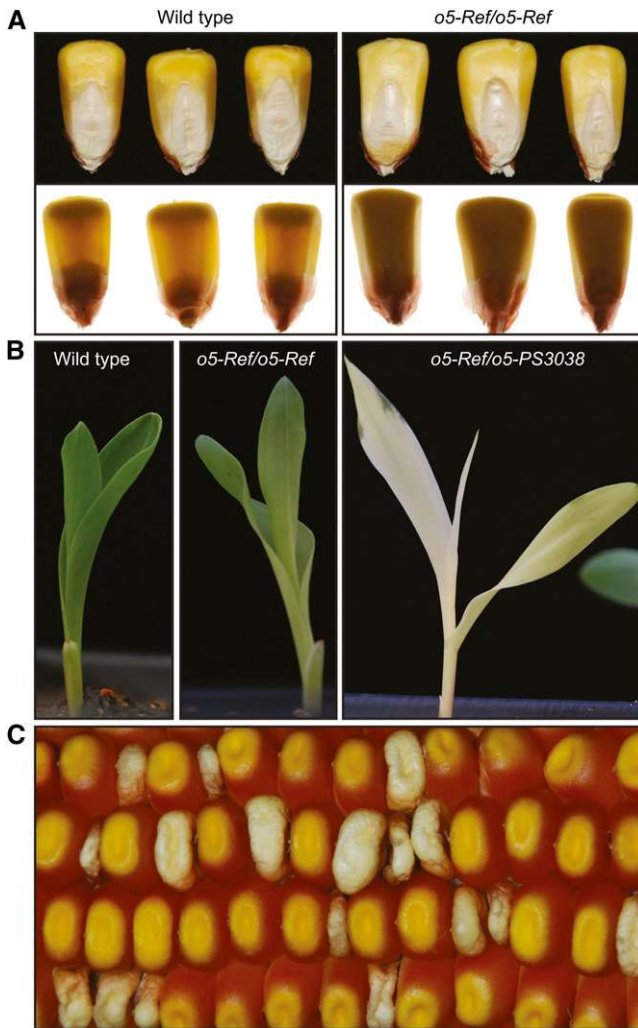


Figure 1. Kernel and Seedling Phenotypes.

(A) *o5-Ref* kernel phenotype. Mature kernels from a self-pollinated ear of an *o5-Ref/+* heterozygote were photographed under reflected light (black background) or backlit by a transilluminator (white background).

(B) Seedling phenotypes. Kernels of the indicated genotype were planted in the greenhouse, and seedlings were photographed 7 d after emergence.

(C) *o5-PS3038* kernel phenotype. A portion of a self-pollinated ear from an *o5-PS3038/+* heterozygote is shown. Homozygous mutant kernels are variable in size, often shriveled, floury in texture, and carotenoid deficient.

number EE189213). Gene-specific primers from this sequence were used in combination with a *Mu*-end primer to amplify that specific *Mu* insertion. Forty-eight additional segregants from the cross were thus analyzed, and perfect cosegregation was observed, indicating this *Mu8* insertion is linked to, and potentially causal of, the *o5-PS3038* mutation (Yi et al., 2009).

The genomic sequence adjacent to the *Mu* insertion associated with *o5-PS3038* is within the locus that codes for a protein annotated as MGDG synthase type A (GenBank accession

number EU954700), referred to here as MGD1. The transcribed region of this gene is located on chromosome 7.02 between nucleotides 117,701,235 and 117,708,502 of the B73 reference genome version 2, which as expected is near or at the inferred position of the *o5* locus (Andorf et al., 2010). *Mu8* is inserted into the first exon, 441 bases 3' to the presumed initiation codon (Figure 2A). The effect of this mutation on the *MGD1* mRNA level was examined by RT-PCR amplification of RNA from wild-type and mutant kernels from an ear of a self-pollinated *o5-PS3038/+* heterozygote. Wild-type samples yielded an obvious amplification product when the PCR primers flanked the insertion site, whereas only a trace signal was evident in the mutant kernels (Figure 2B). Product from mutant kernels was most likely derived from pericarp tissue, which is maternal and, thus, heterozygous for a wild-type *o5* allele. A primer pair located 3' to the *Mu* insertion generated an obvious PCR product in both mutant and wild-type kernels. This suggests spurious transcript initiation from within the *Mu* element, as has been described previously for other *Mu*-induced mutations (Barkan and Martienssen, 1991).

The gene encoding MGD1 was examined in three other *o5*-allelic mutants (see Supplemental Table 1 online). *MGD1* cDNA was amplified by RT-PCR and sequenced from homozygous *o5-Ref*, *o5-5288*, and *o5-313328* plants as well as from wild-type inbreds W64A, Oh43, and B73. Single nucleotide polymorphisms were identified that caused amino acid substitutions specifically in *o5-Ref* and *o5-5288* mutants. In *o5-Ref*, a G/T transversion at nucleotide 1511 (numbering according to GenBank accession number BT042676) would change the residue at position 430 from a Gly to a Cys. This Gly is invariant in MGD coding sequences among vascular plants, moss, and species as divergent as the diatom *Phaeodactylum tricornutum* (see Supplemental Figure 1 online) (Botté et al., 2005). cDNA clones from *o5-5288* seedlings contained two substitutions in *MGD1* relative to the wild type. A G/A transition at nucleotide 504 would cause substitution of the Gly at residue 94 by Asp, and an A/G transition at nucleotide 653 changes the invariant Met codon at position 144 to a Val. Invariant residues are usually essential for protein function, indicating that the nonconservative amino acid substitutions in *o5-Ref* and *o5-5288* are likely to impair MGD1 enzyme activity.

Changes in the gene encoding MGD1 were also detected in plants carrying *o5-313328* (see Supplemental Table 1 online). Homozygotes for *o5-313328* did not display any differences from the wild type in the full-length *MGD1* cDNA sequence; however, genomic DNA contained a deletion of 79 bp in intron 7 that was not detected in any wild-type line. RT-PCR with primers spanning the seventh intron consistently generated decreased amounts of amplification product compared with normal, whereas primers that amplified an alternatively spliced and presumably nonfunctional transcript exhibited an increased signal (Figures 2A and 2C). This suggests that splicing of intron 7 is less efficient than normal owing to the deletion associated with *o5-313328*.

In summary, plants carrying four independent *o5*-alleles were altered in the gene encoding MGD1. Together with the fact MGD1 coding sequences could not be separated from the *o5* locus, the data demonstrate that *o5* codes for MGD1.

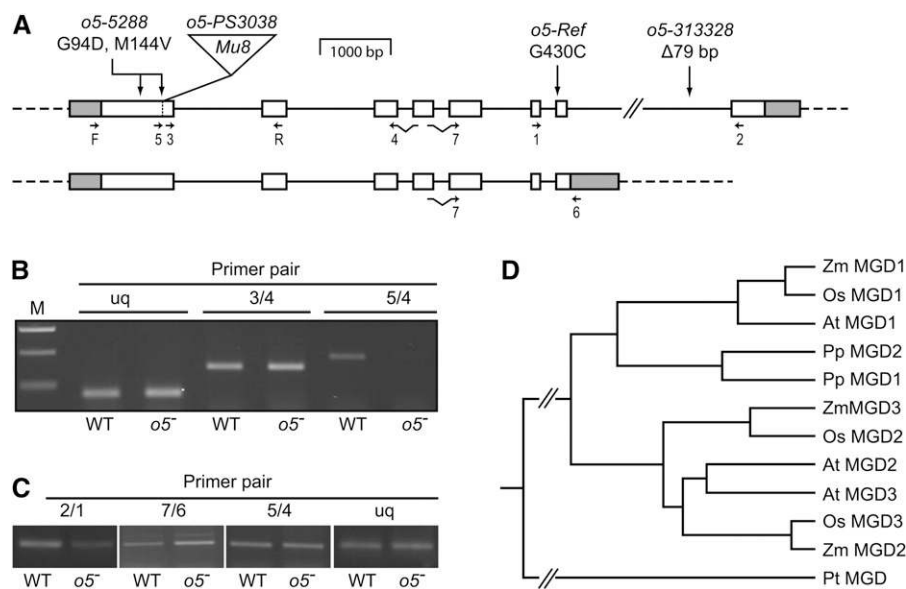


Figure 2. Characterization of the *o5* Locus.

(A) Locus structure. Introns are shown as solid lines, exons as boxes, and untranslated regions as gray boxes. Mutation sites are indicated. Small arrows indicate the locations of oligonucleotide primers used in RT-PCR analyses in **(B)** and **(C)**. The figure is drawn to scale except for intron 7, which is ~3.1 kb. The top diagram maps the transcript that appears most frequently in EST data, and the bottom diagram maps an alternative transcript that fails to remove intron 7 and uses a different 3' end processing site.

(B) Transcript accumulation in *o5-PS3038* kernels. *MGD1* mRNA was detected by RT-PCR in wild-type (WT) and *o5-PS3038/o5-PS3038* kernels (designated *o5*⁻) harvested from a segregating ear at 15 DAP. Primers locations are shown in **(A)**. The ubiquitin (*uq*) gene transcript was used as a positive control. M, molecular weight standards.

(C) Transcript accumulation in *o5-313328* kernels. Analysis as in **(B)**.

(D) Phylogenetic relationship of MGD genes. The *o5* gene product (shown as Zm MGD1) was aligned with MGD proteins from maize, rice, *Arabidopsis*, the moss *Physcomitrella patens*, and the diatom *P. tricornutum*. GenBank protein accession numbers are listed in Methods.

Bioinformatic Analyses

Genomics data (<http://www.plantgdb.org> and <http://www.maizeGDB.org>) revealed that the transcribed region of *o5* spans ~7267 bp, including eight exons and seven introns (Figure 2A). The longest identified mature transcript (GenBank accession number BT042676) comprises 2188 bp with 1589 bp of coding sequence and noncoding regions of 223 and 374 bp at the 5' and 3' ends, respectively. The full-length protein product is predicted to contain 529 amino acid residues, including a 53-residue plastid transit peptide predicted by the TargetP algorithm (Emanuelsson et al., 2007). The predicted molecular mass of mature MGD1 is 51.7 kD.

The full-length amino acid sequence contains a conserved glycosyl transferase (GT) domain classified as family GT28 according to the Carbohydrate Active Enzymes database (Cantarel et al., 2009), whose members are predicted to exhibit the conserved GT-B structural fold (Lairson et al., 2008). This structure comprises residues 151 to 482 of the full-length MGD1 sequence, so an amino terminal extension of ~98 residues is attached to the catalytic domain in the mature protein. The first half of the GT domain is further classified as an MGDG synthase domain, denoted as structure PF06925 in the Pfam database (Finn et al., 2010). Maize MGD1 is 86% identical to *Arabidopsis* MGD1 from residues 137 to 519 of the full-length sequence, with

no gaps in the alignment. Sequence identity between maize and *Arabidopsis* MGD1 from residues 1 to 136 is much less but still significant, with 32% identical amino acids over 120 aligned residues, including four gaps.

o5 is one of three loci in the maize genome coding for predicted MGDG synthases. The other two genes, *mdg2* and *mdg3*, are located on chromosomes 5 and 1, respectively. MGD1 groups phylogenetically with type A MGD synthases, whereas MGD2 and MGD3 are related more closely to type B enzymes (Figure 2D). National Center for Biotechnology Information (NCBI) annotation of the MGD2 and MGD3 genes is discrepant between maize and rice (*Oryza sativa*), hence, the apparent nonconcordance in the phylogeny. As a type A MGD synthase, maize MGD1 would be predicted to be expressed widely throughout the plant. This was tested by RT-PCR amplification of *MGD1* mRNA from seedling shoot, root, juvenile and adult leaf tissue, tassel, ear, kernels at various developmental stages, endosperm harvested 20 d after pollination (DAP), and 20 DAP embryo. Signals were evident in all tissues tested (Figure 3A), supporting classification of MGD1 as a type A enzyme.

Effects of *o5* Mutations on Lipid Constituents

Polar lipids from seedling leaves and developing endosperm were characterized to test whether MGD function is altered in

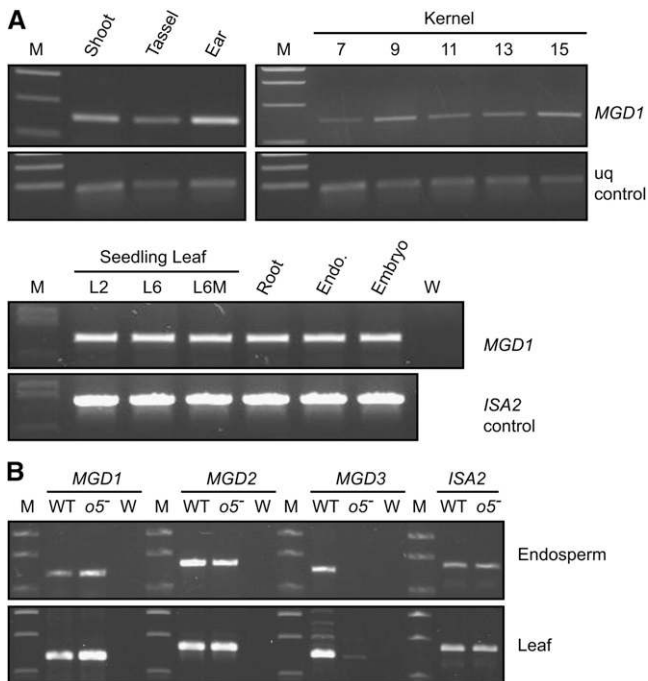


Figure 3. RT-PCR Analysis of Transcript Levels.

(A) Expression of *MGD1* mRNA in wild-type tissues. RNA from the indicated tissues was amplified using primers specific for the *MGD1* transcript. The ubiquitin (*uq*) or *ISA2* transcripts were used as controls. M, molecular weight standards. W, no template control. Shoot and root were from seedlings. Ear tissue was from early development when the organ was ~2 mm in length. Whole kernels were analyzed at the indicated days after pollination. L2, leaf from two-leaf seedlings; L6, youngest leaf of six-leaf seedlings; L6M, mature seedling leaf defined as the outer one-third of the third leaf of six-leaf seedlings. Endosperm and embryo were from kernels harvested 20 DAP. In the top panel, primers 3 and 4 were used to amplify cDNA, and in the bottom panel, the primers were F and R. The locations of the primers are shown in Figure 2A.

(B) Expression of *MGD1*, *MGD2*, and *MGD3* mRNAs in wild-type and *o5-Ref* tissues. Total RNA from endosperm or leaf was amplified using primers specific for the indicated transcript. The *ISA2* transcript provided a positive control. M, molecular weight standards; WT, wild-type inbred W64A; *o5*⁻, plants homozygous for *o5-Ref*; W, no template control.

o5⁻ mutants and to further define the effects of these mutations. Organic extracts were analyzed by mass spectrometry to identify and quantify individual phospholipids and galactolipids (Welti and Wang, 2004) (complete data set in Supplemental Data Set 1 online). The molar percentage of total galactosylglycerol (GDG) was ~42% in wild-type endosperm, whereas in seedlings, the GDG content was ~92% (Figure 4A). The distribution between MGDG and DGDG differed between the tissues, with monogalactosyl species constituting approximately one-third of total GDG in endosperm and two-thirds in seedling leaves (Figure 4A). The great majority of GDG in both endosperm and leaf were C₁₈/C₁₈ species (Figure 4B), and thus are expected to be derived from the ER assembly pathway (Benning, 2008). Among the C₁₈/C₁₈ GDG species, there were major differences between wild-type tissues in the degree of desaturation of the acyl groups.

Endosperm contained predominantly 36:4 lipid, with ~13% 36:5 species and essentially no 36:6 lipids. Leaf tissue, conversely, contained predominantly 36:6 GDG species and very little 36:4 lipid. The 36:5 GDG content was similar in leaf and endosperm (Figure 4B).

Total GDG content in endosperm was reduced approximately fourfold in homozygous *o5-Ref* mutants compared with the wild type (Figure 4A), supporting the conclusion that *o5* codes for MGDG synthase. Both MGDG and DGDG abundance were reduced by the mutation. The distribution between 36:4 and 36:5 GDG was essentially unchanged in wild-type and *o5-Ref* endosperm (see Supplemental Data Set 1 online).

In contrast with endosperm, the total GDG level in leaves was not significantly altered in *o5-Ref/o5-Ref* homozygotes and was only slightly reduced when one copy of *o5-Ref* was present along with one copy of the null allele *o5-PS3038* (Figure 4A). Thus, reduced total GDG level is not likely to be the cause of the leaf phenotypes. However, significant changes were noted in the abundance of 36:5 GDG species between the wild type and mutants. The total abundance of C₁₈/C₁₈ GDG was the same in W64A and *o5-Ref* leaves; however, the mutant had approximately one-half the wild-type amount of 36:5 GDG (Figure 4C). Heteroallelic *o5-Ref/o5-PS3038* leaves had one-quarter of the wild-type 36:5 GDG content. Thus, the magnitude of the effect was proportional to dosage of partially functional alleles at the *o5* locus. This effect was observed for both 36:5 MGDG and 36:5 DGDG (see Supplemental Data Set 1 online).

Proportionality to functional gene dosage, and accordingly to phenotypic severity, was observed only for 36:5 GDG content. Other changes in polar lipid abundance were observed; however, these were quantitatively small and did not correlate with phenotype. For example, MGDG abundance was reduced slightly but significantly in both mutant lines compared with the wild type (Figure 4A). This is not the cause of the leaf phenotypes because the total MGDG level was the same in *o5-Ref/o5-Ref* and *o5-Ref/o5-PS3038* plants, although they display very different leaf phenotypes. Changes in phospholipid content between mutant and wild-type leaves also were observed (see Supplemental Data Set 1 online); however, these are minor species comprising in total <10% of the polar lipids. Proportionality to gene dosage or phenotype was not observed for any change in phospholipid content.

Expression of MGD Genes in Endosperm and Leaf

The greater effect of *o5*⁻ mutations on total GDG level in endosperm than leaf could be explained by a compensation mechanism in the latter tissue. One possibility is that *mgd2* or *mgd3* expression is induced in *o5*⁻ mutant leaf tissue but not in endosperm. This was investigated by examining the levels of transcripts coding for MGD using RT-PCR. *MGD1*, *MGD2*, and *MGD3* transcripts were all present in both leaf and endosperm of wild-type plants (Figure 3B). The *MGD1* mRNA level was not altered in either tissue by *o5-Ref*, consistent with identification of that allele as a point mutation. In both leaf and endosperm, *MGD2* mRNA was present at the same levels in *o5-Ref* mutants as in the wild type. *MGD3* mRNA was strongly reduced in concentration as a result of *o5-Ref* in both leaf and endosperm. The

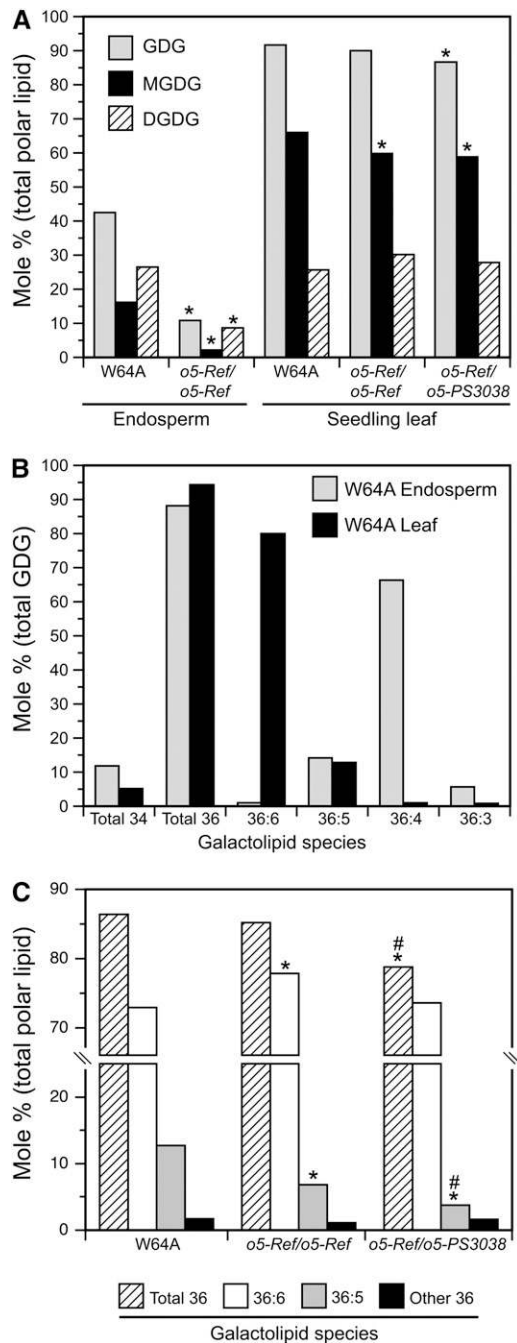


Figure 4. Lipid Content.

(A) Galactolipid species abundance in leaf and endosperm of the wild type and *o5-* mutants. MGDG, DGDG, and total GDG abundance is plotted as the molar percentage of total polar lipid. Values are averages of independent biological replicates (W64A endosperm, $n = 4$; *o5-Ref/o5-Ref* endosperm, $n = 5$; all seedling leaf tissue, $n = 3$; $SD \leq 2.1\%$). Asterisks indicate significant differences from the wild type ($P < 0.01$; Student's t test). Differences between *o5-Ref/o5-Ref* and *o5-Ref/o5-PS3038* were not observed at this level of significance.

(B) Degree of desaturation in galactolipids of wild-type leaf and endosperm. Galactolipid species abundance is plotted as the molar percent-

age of total galactolipid. Independent replicates were as in **(A)** ($SD \leq 0.6\%$).

reason *o5-Ref* would affect *MGD3* expression is not clear; however, the data taken together are inconsistent with the hypothesis that increased expression of *MGD2* or *MGD3* mRNA is the reason that *o5-Ref* has relatively little effect in leaf. The possibility remains that *MGD2* functions in leaf but not in endosperm, despite the fact that the mRNA is present in both tissues.

Effects of *o5* Mutations on Kernel Development

Endosperm characteristics were examined to investigate the nature of the opaque kernel phenotype. Homozygous *o5-Ref* mutants are viable, and mature kernels appeared normal except for the loss of translucency typical of wild-type maize seed (Figure 1A). Starchy endosperm tissue at mid-development (20 DAP) was abnormal, with highly vacuolated cells containing decreased numbers of starch grains that were noticeably smaller than the wild type (Figure 5A). At maturity, starch granule size in *o5-Ref* endosperm was similar to the wild type, although they appeared less densely packed and often compound (Figure 5B).

Homozygous *o5-PS3038* mutants exhibit a defective kernel phenotype in which the seeds are small, white, collapsed to varying degrees, and have poorly developed, floury endosperms (Figure 1C). Homozygous mutant endosperm cells at 15 DAP had greatly decreased cellular contents and displayed a variety of cytological abnormalities, such as amoeboid nuclei and undefined globular structures (Figure 5A). At maturity, starch granules were evident in many cells, although they often showed highly irregular morphologies, including a dramatic enlargement and high degree of compounding (Figure 5B). Also of note were contiguous zones of cells devoid of starch grains or other recognizable structures (Figures 5A and 5B). These vacant zones, observed at both mid-development and maturity, were not seen in wild-type endosperm. Transmission electron microscopy (TEM) analysis revealed that cells in these zones were filled with many small vesicles and other bodies of unknown composition (Figure 5B).

Wild-type and mutant endosperm and starch granules were further examined by TEM (Figure 6). Normal tissue revealed characteristic simple granules surrounded individually by amyloplast envelope. The compound nature of starch in mature *o5-PS3038* mutant endosperm was clearly evident in TEM, with internal membranes separating individual granules packed together within a single amyloplast. Entire compound granules were surrounded on the exterior with plastid envelope. Each particle within a single plastid displayed concentric growth rings, demonstrating compound granules derived from multiple initiation events rather than fractured simple granules. Growth rings

age of total galactolipid. Independent replicates were as in **(A)** ($SD \leq 0.6\%$).

(C) Comparison of the degree of desaturation in galactolipids of wild-type and *o5-* mutant leaves. Galactolipid species abundance is plotted as the molar percentage of total polar lipid. Independent replicates were as in **(A)** ($SD \leq 1.6\%$ for all samples and $\leq 0.6\%$ for 36:5 species). Asterisks indicate significant differences from the wild-type value, and pound signs indicate significant differences from the *o5-Ref/o5-Ref* value ($P < 0.01$; Student's t test).

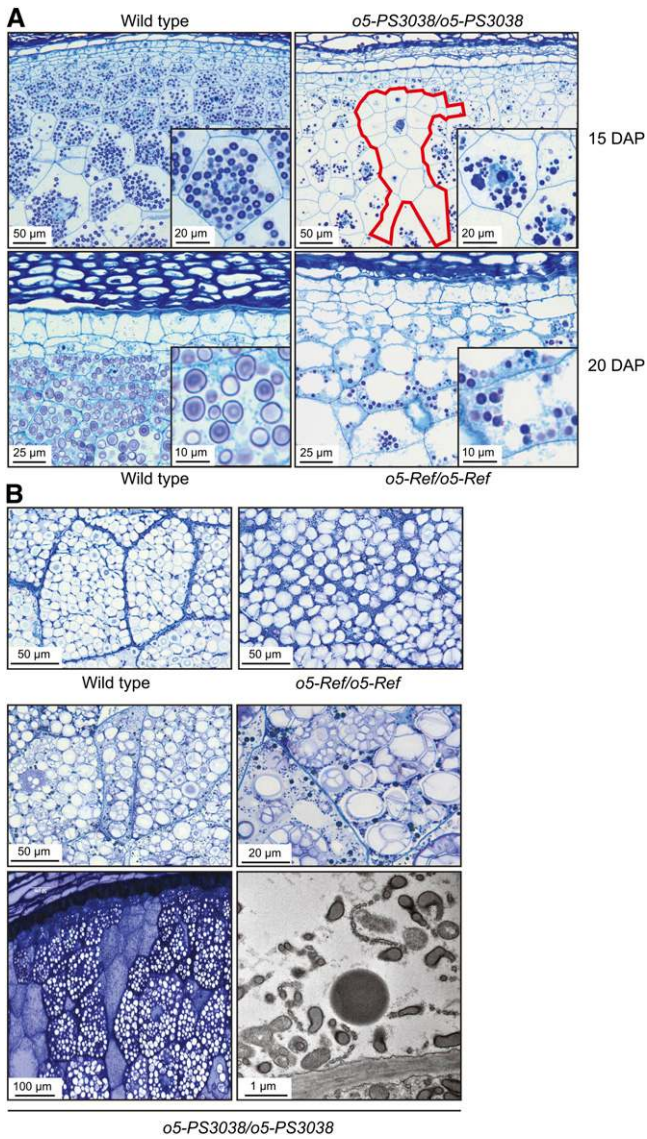


Figure 5. Endosperm Development.

(A) Histological sections of immature endosperm. Wild-type and mutant kernels were collected at 15 DAP from a self-pollinated *o5-PS3038/+* plant and at 20 DAP from a self-pollinated *o5-Ref/+* plant. A cluster of cells in *o5-PS3038/o5PS3038* endosperm largely devoid of starch grains is outlined in red.

(B) Histological sections of mature endosperm. Mature kernels were collected from the plants described in **(A)** and either fixed for histological analysis by light microscopy or embedded, thin-sectioned, and analyzed by TEM (bottom right panel). The TEM image depicts a cell from a region of *o5-PS3038/o5PS3038* endosperm devoid of starch granules (bottom left panel).

in mutant starch grains appeared to be irregularly spaced compared with the uniform rings in wild-type granules. Mature *o5-Ref/o5-Ref* endosperm observed in TEM also exhibited numerous compound granules but less frequently than in the null mutant. These also were surrounded on the exterior by amyloplast envelope, with interior membranes separating individual

particles (Figure 6). Most granules in *o5-Ref* tissue were close to the wild type in size and growth ring spacing.

Embryo development was also severely affected in homozygous *o5-PS3038* mutants. Longitudinal sections of developing kernels harvested 15 DAP revealed that the mutant embryos attained a relatively normal transition stage morphology but failed to progress further (Figure 7). Wild-type embryos had established an axis, shoot apical meristem, and scutellum by this point.

Effects of *o5* Mutations on Starch Biosynthesis

Morphological abnormalities of starch granules in *o5⁻* mutants prompted more detailed investigation of starch biosynthesis. Consistent with fewer and smaller starch granules in *o5-Ref* endosperm at mid-development compared with the wild type

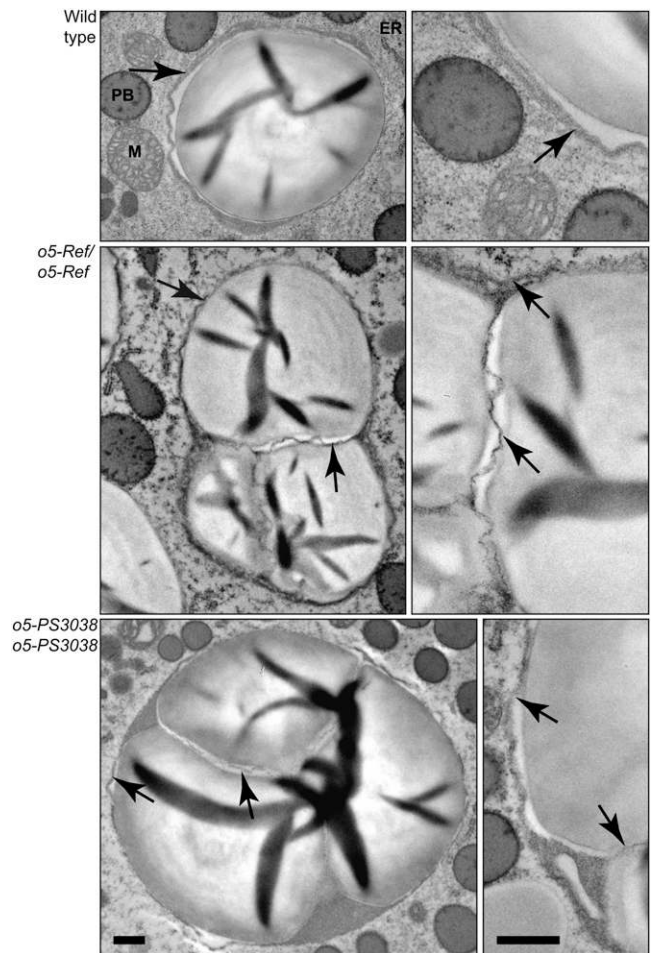


Figure 6. TEM Visualization of Mature Starch Grains in Endosperm Tissue.

Kernels on self-pollinated ears of *o5-Ref/+* or *o5-PS3038/+* heterozygotes were harvested at maturity, fixed, thin-sectioned, and analyzed by TEM. Dark-staining areas within granules are folds that arise during sectioning. Arrows indicate amyloplast envelope or internal membrane. Bars = 0.5 μ m and apply uniformly within each column. Organelles are indicated: M, mitochondria; PB, protein bodies.

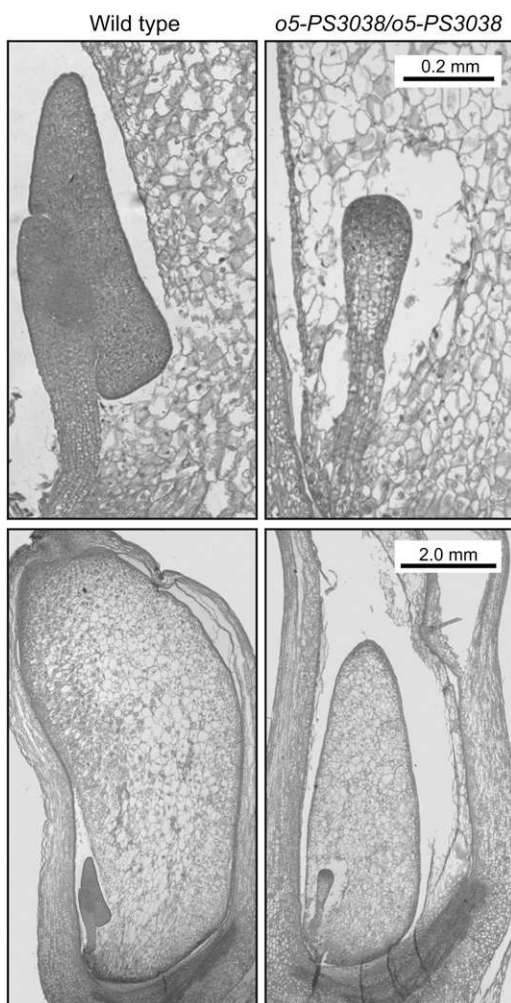


Figure 7. Embryo Development.

Wild-type and homozygous *o5-PS3038* kernels harvested from a segregating ear at 15 DAP were collected, and longitudinal sections were prepared such that both endosperm and embryo were included. Tissue sections were stained with Safranin O and fast green. Bars apply to both images in each row.

(Figure 5A), the total starch content measured at 20 DAP was significantly reduced in the mutant ($P = 0.02$; Table 1). Water-soluble polysaccharide was elevated in the mutant at this stage by approximately sixfold compared with the wild-type level. By contrast, at maturity when *o5-Ref* starch granules are generally similar in size to the wild type (Figure 5B), neither the total starch content nor the water-soluble polysaccharide level was significantly altered in the mutant (Table 1). Amylose content was the same in mature starch granules from wild-type or *o5-Ref/o5-Ref* endosperm (Table 1).

Glucan chain length distribution in amylopectin from *o5-Ref* and wild-type endosperm was determined using fluorophore-assisted carbohydrate electrophoresis (Morell et al., 1998; O'Shea et al., 1998). Biological replicates of starch from kernels harvested 20 DAP showed that the measured chain length

distribution was highly reproducible for both wild-type and *o5-Ref* homozygotes (Figure 8). Compared with B73 or W64A wild-type starch, *o5-Ref* starch had an elevated frequency of linear chains with degrees of polymerization in the 12 to 21 range. The chain lengths that are increased in frequency constitute the crystalline lamellae of amylopectin (Buléon et al., 1998).

The assembly state of isoamylase-type starch debranching enzymes (ISA) was analyzed because mutations affecting these enzymes change amylopectin chain length frequency in the same size range that is altered in *o5-Ref* mutants (Dinges et al., 2001). Three bands of ISA activity are observed in extracts of 20 DAP wild-type endosperm after native-PAGE, electrophoretic transfer to a starch-containing gel, and then staining with I_2/KI (Kubo et al., 2010). Endosperm of *o5-Ref* kernels reproducibly exhibited a fourth band of ISA activity (Figure 9). The levels of ISA1 and ISA2 protein determined by immunoblot analysis using isoform-specific IgG fractions were the same in *o5-Ref* and wild-type endosperm. Multiple ISA activity bands are known to result from different assembly states of the ISA1 and ISA2 proteins in multimeric complexes in both maize and rice (Utsumi and Nakamura, 2006; Kubo et al., 2010). The data suggest that the change in membrane lipid composition caused by *o5-Ref* results in altered assembly of one or more of these ISA complexes.

Mutations of *o5* Disrupt Chloroplast Structure

Further microscopy characterization of photosynthetic tissue was undertaken to investigate the nature of the pale-green or colorless seedling phenotype observed in viable *o5-Ref* homozygotes or seedling-lethal *o5-Ref/o5-PS3038* compound heterozygotes (Figure 1B). The *o5-Ref* mutant leaves in cross section appear similar to the wild type with regard to the number of chloroplasts present in mesophyll and bundle sheath cells. The chloroplasts appear less tightly appressed to the periphery of mutant bundle sheath cells than in the wild type (Figure 10). The number of chloroplasts present in the more severely affected *o5-Ref/o5-PS3038* seedlings is noticeably reduced from the wild type, particularly in mesophyll cells.

TEM observation of individual chloroplasts revealed defects in membrane assembly that increased in severity proportional to the reduction in 36:5 galactolipid content (Figure 10). Highly organized granal stacks of thylakoid membranes were clearly observed in chloroplasts of wild-type mesophyll cells. Chloroplasts in *o5-Ref/o5-Ref* mesophyll had less extensive grana, and this effect was more severe in *o5-Ref/o5-PS3038* plastids where

Table 1. Endosperm Carbohydrate Content

Genotype	20 DAP		Mature		
	Starch	WSP	Starch	WSP	Amylose (%)
+/+	697 ± 74	4.0 ± 1.1	598 ± 51	3.3 ± 1.1	22
<i>o5-Ref/o5-Ref</i>	502 ± 45	23.1 ± 2.0	563 ± 27	3.0 ± 1.0	25

Starch and water-soluble polysaccharide (WSP) content is expressed as mg/g dry weight. Values are the mean ± SD from three biological replicates. Amylose content is expressed as the percentage of total carbohydrate in purified starch.

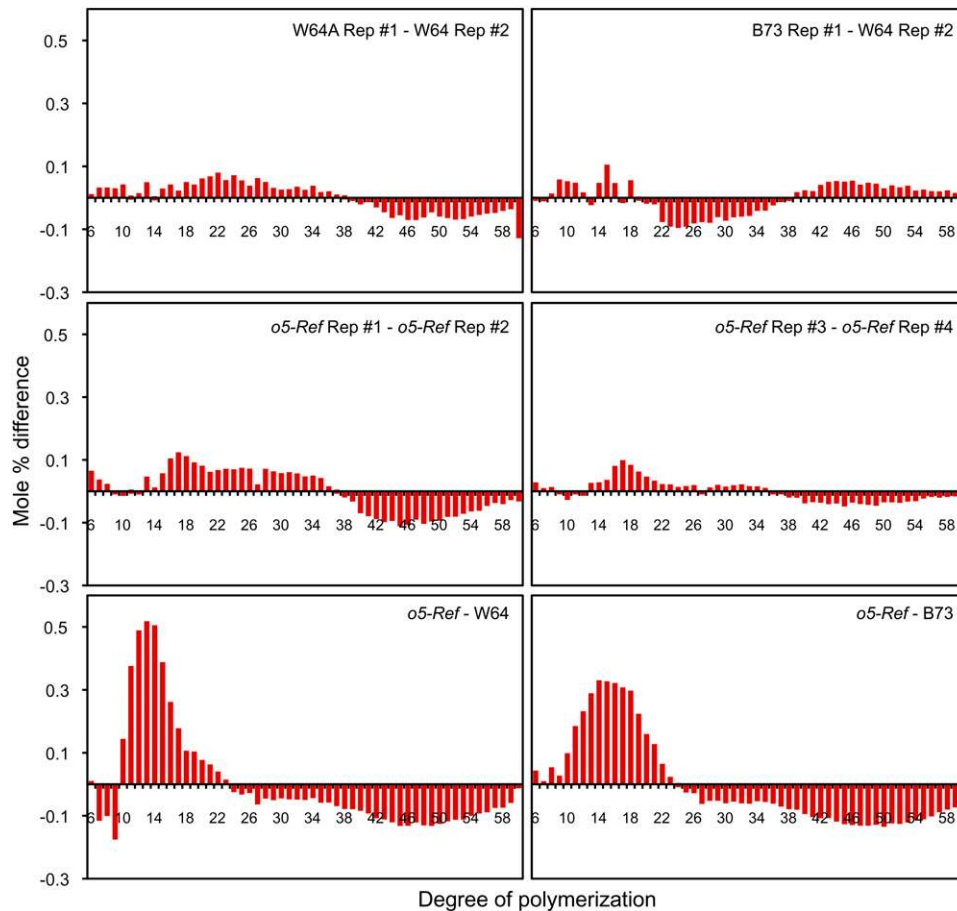


Figure 8. Amylopectin Chain Length Distribution.

Total starch from the indicated genotypes was debranched with commercial isoamylase, and mole percentage of linear chains of each degree of polymerization was normalized to the total number of chains from DP5 to DP48. Plots show the difference between the mole percentage of each chain length for the two indicated lines. The designations #1, #2, etc., indicate independent biological replicates of the same genotype. For comparison between genotypes (bottom row), the average values for four independent replicates of the mutant and two independent replicates of each wild-type inbred line were compared.

[See online article for color version of this figure.]

internal membrane structure appeared sparse and even less organized (Figure 10). Normal bundle sheath chloroplasts also possess an organized thylakoid membrane system although they lack grana and are the major sites of transient leaf starch accumulation. The thylakoids in chloroplasts of *o5-Ref/o5-PS3038* bundle sheath cells showed decreased lamellar structure, and starch grains were rare and much smaller (see Supplemental Figure 2 online).

DISCUSSION

o5 Encodes a Type A MGDG Synthase

The combined genetic and biochemical analyses presented here make clear that the maize *o5* gene encodes a type A MGD synthase. A specific transposon within the gene that codes for

MGD1 was genetically inseparable from a defined *o5* mutation. Furthermore, plants carrying any of three additional independent *o5* alleles also contained specific mutant variants at the locus encoding MGD1. Accumulation of direct and indirect products of MGD1 (i.e., MGDG and DGDG, respectively) is strongly reduced in endosperm tissue in mutants carrying lesions in *o5*. Taken together, these data demonstrate that MGD1 defects are the causative agents of the observed phenotypes in *o5* mutants.

Galactolipids in Maize Endosperm and Leaf

Wild-type leaf and endosperm varied considerably in galactolipid content in three aspects. First, seedling leaves contained >90% GDG as a molar percentage of total polar lipids compared with 42% of total in endosperm. Second, MGDG abundance relative to DGDG was different in the two tissues, with approximately one-third of the total GDG as monogalactosyl forms in



Figure 9. Starch Modifying Enzymes.

Extracts of 20 DAP endosperm were separated by native-PAGE and analyzed by zymogram. Differential color staining in I_2/KI revealed changes in starch structure owing to specific enzyme activities. Blue bands result from ISA complexes and red bands from starch branching enzymes. ISA form I is known to be an ISA1 homomeric complex, whereas forms II and III are ISA1/ISA2 heteromers. The asterisk indicates the position of an ISA activity observed reproducibly in *o5-Ref* endosperm that is not seen in the wild type.

endosperm and two-thirds in leaf. Finally, the degree of desaturation was very different. About 67% of endosperm GDG was a 36:4 species (i.e., 18:2 fatty acyl groups at both the sn-1 and sn-2 positions), and this tissue was essentially devoid of 36:6 species. By contrast, leaf comprised $\sim 80\%$ 36:6 species, whereas 36:4 GDG was detected at only a trace level. These endosperm characteristics are consistent with previous characterization of potato (*Solanum tuberosum*) amyloplast membranes, which showed DGDG in excess of MGDG, and preponderance of 18:2 fatty acids relative to 18:3 species in all galactolipids (Fishwick and Wright, 1980).

Maize leaf GDG content was high relative to that reported for other plant species (e.g., 60 to 70% in *Arabidopsis* leaves) (Dörmann et al., 1995; Jarvis et al., 2000). This discrepancy could be explained by differences in developmental stage, inherent species characteristics, or possibly the use of mass spectrometry as the detection method in this study. Regardless, GDGs are the major polar lipids present in both maize and *Arabidopsis* leaves. Maize GDG has $\sim 95\%$ C_{18}/C_{18} species thought to derive from the eukaryotic pathway of GDG biosynthesis. Previous reports indicated that maize was devoid of C_{18}/C_{16} GDG species (Mongrand et al., 1998 and references therein); however, the use of mass spectrometry now reveals that a minor amount of GDG biosynthesis proceeds through the prokaryotic pathway in both maize leaves and endosperm.

Unique Effects of *o5*⁻ Mutations on Leaf Galactolipids

This study characterized the effects of disrupted *MGD1* function in maize, a monocot species that uses the C4 photosynthetic pathway. The *o5*⁻ alleles affected lipid content in ways that were not seen previously in analysis of *mgd1* mutants in *Arabidopsis* (Jarvis et al., 2000; Kobayashi et al., 2007), thus providing insight into functions of specific lipid species. In mutant maize leaves, the reduction in total GDG content was much less severe than that observed in *Arabidopsis*, even though in both instances chlorotic phenotypes were observed. Notably, there was no

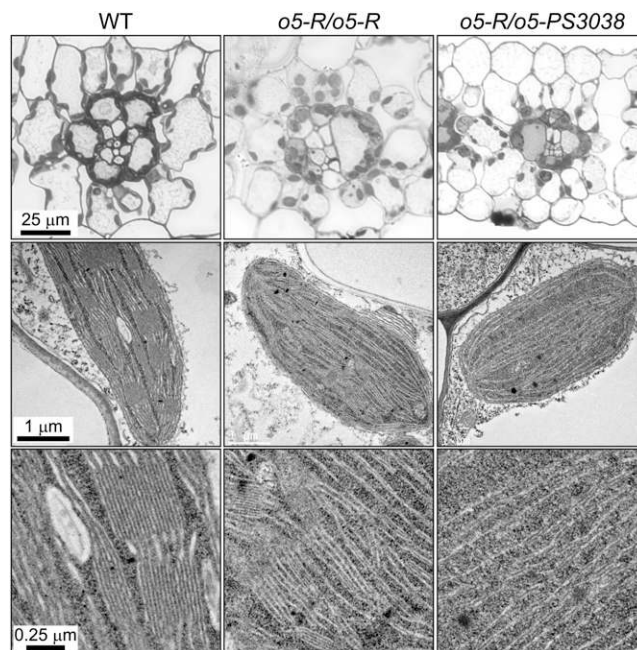


Figure 10. Effects of *o5*⁻ Mutations on Leaf and Chloroplast Morphology.

Seedling leaves were fixed and sectioned for either light microscopy or TEM. The top row shows chloroplasts as dark staining bodies that appear contiguous in the bundle sheath cells. Individual mesophyll chloroplasts visualized by TEM are shown in the bottom two rows. Bars apply uniformly within each row. WT, wild type.

significant difference in total GDG content between W64A and homozygous *o5-Ref* leaves. In *o5-Ref/o5-PS3038* compound heterozygotes, which are severely chlorophyll deficient, the total GDG decrease was 5% of the wild-type value. This compares to a total GDG decrease of 20% in hypomorphic *Arabidopsis mgd1-1* mutants. With regard to MGDG specifically, mutant maize seedlings were reduced by <11% compared with the 42% reduction seen in *Arabidopsis*. Thus, the data reveal that photosynthetic development can be impaired as the result of less severe and more specific changes in the GDG profile than have been observed previously.

Further analysis revealed that 36:5 galactolipids are specifically required for normal chloroplast structure and function and that this requirement cannot be substituted by 36:6 species. There was clear correspondence between the level of MGD1 function and 36:5 GDG content. The *o5-Ref/o5-Ref* line with two copies of the hypomorphic point mutation showed 50% reduction in 36:5 GDG compared with the wild type, whereas *o5-Ref/o5-PS3038*, with one copy of the hypomorphic allele and one null allele, was reduced 75%. Successively greater reduction in 36:5 GDG corresponded to the increasing phenotypic severity of the two mutant lines. No other parameters of lipid content exhibited such correspondence. Taken together, the data are strong evidence that 36:5 GDG deficiency causes the photosynthetic defects.

The specific reduction in 36:5 galactolipids, and not 36:6 lipids, indicates molecular recognition of acyl group structure on the DAG acceptor substrate by MGD synthase(s). Galactolipid precursors with 36 carbons in the acyl groups are provided from the ER lipid assembly pathway with alkene groups already in place, prior to conversion to DAG in the plastid and subsequent glycosylation by MGD1 (Benning, 2008). Thus, reduction in 36:5 GDG content but not 36:6 GDG most likely is explained at the level of the galactosyl transferase. The alternative is that *o5* mutations affect fatty acyl desaturases in the ER, which is implausible given the enzymatic function of MGD1 and its location in the inner plastid envelope. Both MGDG and DGDG were reduced in 36:5 frequency to the same extent, suggesting that DGDG synthase activity is not affected by the desaturation state of the DAG substrate. This observation is consistent with the fact that MGDG produced by MGD1 in the inner envelope is the substrate of DGD1 and DGD2 located in the outer envelope membrane (Kobayashi et al., 2007; Benning, 2008).

The relatively small change in galactolipids in *o5-Ref/o5-Ref* or *o5-Ref/o5-PS3038* leaves could result from inherent properties of the G430C mutant MGD1 enzyme and/or by compensatory activity of another MGD synthase(s). MGD1-G430C could be altered in enzymatic rate or substrate binding but not devoid of function, so that MGDG synthesis is reduced but not eliminated. This is likely because seedlings with two copies of *o5-Ref* apparently attain full photosynthetic capacity, whereas those with only one copy remain chlorotic and are inviable, and because 36:5 GDG content increases with two copies of the mutant allele relative to only one copy. These observations are consistent with the hypothesis that MGD1-G430C is impaired in recognition of 36:5 DAG as a substrate but not 36:6 DAG. Based on molecular modeling studies, G430 is predicted to be located within the active site of MGD1, near the sites involved in binding to both the

UDPGal donor and the DAG acceptor substrate (Botté et al., 2005). Thus, perturbation of DAG substrate selection owing to the G430C mutation is plausible.

The possibility also exists that MDG2 could be active in maize seedling leaves so that loss of MGD1 activity has only a small effect on total MGDG synthesis. According to this hypothesis, the MGD2 enzyme would have reduced activity toward 36:5 DAG substrates relative to 36:6 DAG. *MGD2* mRNA is present in seedling leaves, at the same level in either *o5* or wild-type plants. MGD3 can be ruled out as a compensating enzyme because the corresponding transcript is not detected in mutant leaves. MGD2 activity cannot fully explain the slight changes in GDG levels, however, because such compensation should occur to the same extent regardless of whether one or two copies of *o5-Ref* are present. Compensation clearly does not occur in *Arabidopsis* because an *mgd1* null mutation caused essentially complete absence of GDG in seedlings even though MDG2 and MDG3 transcripts were present (Kobayashi et al., 2007). Thus, partially reduced activity of the mutant MGD1 encoded by *o5-Ref* is responsible for the specific lipid phenotype, at least to some extent if not entirely.

Galactolipid Function in Chloroplasts

The *o5-Ref/o5-PS3038* seedlings exhibited altered chloroplast structure attributed to deficiency of 36:5 GDG. The observed morphological defects in the plastid are more severe than those caused by the hypomorphic allele *mgd1-1* in *Arabidopsis* (Jarvis et al., 2000) despite much smaller changes in MGDG or total GDG content. In the dicot, the amount of thylakoid membrane was substantially decreased, although the remaining membranes formed morphologically normal granal stacks. By contrast, *o5-Ref/o5-PS3038* mesophyll thylakoid membrane structure was drastically altered such that normal grana were lost. An intermediate degree of thylakoid disorganization was observed in *o5-Ref/o5-Ref* mesophyll, supporting the conclusion that 36:5 GDG content is the determining factor. The extensive granal stacks of mesophyll thylakoid membrane are enriched in photosystem II complexes, and assembly of these complex structures apparently requires a minimal amount of 36:5 MDGD and/or 36:5 DGDG. Formation of grana is not the only membrane process that requires 36:5 GDG, however, because loss of integrity in the internal membranes of bundle sheath chloroplasts, as well as mesophyll plastids, was evident in *o5* seedlings. Mesophyll and bundle sheath chloroplasts in C4 plants such as maize exhibit discrete structural features and carry out different biochemical functions. Bundle sheath chloroplasts lack grana and are specialized for carbon fixation in the stroma by the Calvin cycle (reviewed in Waters and Langdale, 2009). Thus, there appears to be a generalized requirement for 36:5 lipids in thylakoid membrane biogenesis that is not restricted to any particular aspect of photosynthesis.

A possible explanation for the function of 36:5 GDG in chloroplasts is that they have a structural organization that differs from that of 36:6 GDG, and lipids with these different properties are necessary for proper thylakoid structure and/or assembly of protein complexes therein. Although most membrane lipids are organized in a bilayer structure, MGDG typically assumes a

nonbilayer, reverse hexagonal phase organization (H_{II}) (Cullis and de Kruijff, 1979). Such nonbilayer structures are thought to be particularly suited for tight turns in membranes and/or for packing of membrane around densely populated protein complexes (Simidjiev et al., 2000; Dörmann and Benning, 2002; Hölzl and Dörmann, 2007). Previous research showed that the extent of desaturation affects the propensity of MGDG to adopt the H_{II} structure, such that fewer double bonds favor bilayer formation. Notably, changes from five or more double bonds to less than five can significantly affect the bilayer/ H_{II} distribution (Gounaris et al., 1983). Thus, the effects of $\omega 5^-$ mutations on 36:5 GDG abundance may have changed the abundance and/or location of bilayer and nonbilayer structures within the thylakoids. This in turn could explain the disorganized membranes, loss of granal stacks, and reduced chlorophyll in $\omega 5^-$ leaves.

Galactolipid Function in Amyloplasts

The results of this study provide strong support for the conclusion that a functional connection exists between starch biosynthesis and the structure of internal amyloplast membranes. In contrast with leaves, total GDG content was strongly reduced in endosperm of $\omega 5^-$ homozygotes, to $\sim 25\%$ of normal, and all species of MGDG and DGDG were significantly decreased. Two explanations for the quantitatively different effects between leaf and endosperm can be considered. First, MGD2 or MGD3 activity may compensate for loss of MGD1 in leaf, but not in endosperm. This is unlikely, however, because there are no differences in *MGD2* or *MGD3* mRNA levels between endosperm and leaf in the wild type or $\omega 5^-$ mutants and because, as noted previously, *\omega 5^-* gene dosage clearly determines significant components of the leaf lipid profile. A second explanation could again be that the mutant MGD1 protein differentially recognizes DAG substrates based on degree of desaturation. In contrast with the leaf, endosperm contains virtually no 36:6 GDG species, whereas 36:4 GDG is predominant. If MGD1-G430C is less active against 36:5 DAG than 36:6 DAG, as proposed for leaf, it might be even less active using 36:4 DAG as the substrate. This could explain why the decrease in total GDG is much more severe in endosperm than in leaf.

Reduced GDG content in endosperm membranes had a clear effect on starch, which is likely the reason for the opaque kernel phenotype. At mid-development, granules were smaller in $\omega 5^-$ *Ref* and $\omega 5^-$ *PS3038* homozygous endosperm than in the wild type, suggesting a delay in initiation and/or slower growth rate. Irregular growth ring spacing was observed in mutants, which could reflect altered granule growth processes or may be a consequence of distorted granule shape. Compound granules were frequent in mature mutant endosperm. In the null mutant, almost every granule was compound, and in some instances, there appeared to be 10 or more separate initiation events within the compound granules. Distinct initiation events, as opposed to fractured granules, were demonstrated by TEM observation of separate sets of concentric growth rings.

Little is known about initiation of starch granules in plants in general and endosperm in particular. One clue comes from observations that granule initiation in maize, oat (*Avena sativa*), or barley (*Hordeum vulgare*) endosperm occurs in plastids contain-

ing internal thylakoids, possibly within pockets of such membranes (Buttrose, 1960; Badenhuizen, 1969). Based on such ultrastructural data, association with thylakoid-like membranes within amyloplasts has been proposed as a functional aspect of starch polymer synthesis, granule formation, and growth (Salema and Badenhuizen, 1967; Barlow and Sargent, 1978). Direct evidence addressing this hypothesis is lacking; however, this study provides some support by showing a drastic switch in granule complexity when membrane lipids are altered. In normal maize, granules are first observed in endosperm within elongated, irregularly shaped amyloplasts containing multiple starch particles. Granules grow as development proceeds, and during this period, the amyloplasts divide such that each starch particle is surrounded individually by a double membrane (Badenhuizen, 1969; Shannon et al., 2009). The switch to compound granules in endosperm reduced in GDG content could arise from changes in the amyloplast division process such that membranes are unable to completely separate the growing starch particles. In this instance, outer envelope membrane would surround multiple starch grains, separated from each other by internal plastid membrane. Compound granules are the norm in rice endosperm, where internal membrane is thought to form separate compartments within a single amyloplast, each containing an individual starch particle (Yun and Kawagoe, 2010). Growth of the particles results in a compound granule within each plastid, similar to those observed here in $\omega 5^-$ mutants.

Another interpretation is that abnormal thylakoid membrane structure could affect the temporal or spatial details of granule initiation during the early stages of amyloplast development, so that later separation into individual simple granules does not occur normally. Internal membrane structure may also influence or organize the coordinated activities of starch biosynthetic enzymes. This hypothesis is proposed as an explanation of the alteration in amylopectin fine structure observed to result from decreased GDG content (Figure 8). Amylopectin structure is determined by the combined activities of starch synthases, starch branching enzymes, and starch debranching enzymes (Myers et al., 2000; Ball and Morell, 2003; Zeeman et al., 2007). The functions of one or more of these enzymes could be affected by the structure of amyloplast thylakoids, thus resulting in alterations in granule gross morphology, initiation, growth rate, and/or fine structure. Abnormal assembly of ISA complexes in $\omega 5^-$ *Ref* endosperm is consistent with this hypothesis. The specific connection between GDG content, amyloplast thylakoid structure, and starch biosynthesis currently is not known, although the data of this study indicate clearly that such a connection does exist.

The possibility must be considered that lipid composition indirectly affects starch granule formation. For example, $\omega 5^-$ mutations may impact the plastid import systems, and disrupted protein or metabolite transport could secondarily cause defects in granule production. This explanation is unlikely, however, because amyloplasts in $\omega 5^-$ *Ref* mutants appear to be fully functional in terms of starch level, and mature kernels are viable without germination defects. Altered protein import into amyloplasts would have global effects on metabolism, including starch biosynthesis, and significant changes in metabolite transfer would have similarly broad effects, including decreased total

starch level. Indirect effects of MGD1 deficiency owing to changes in gene expression should also be considered. As with all opaque mutants studied, numerous changes in gene expression at the level of mRNA accumulation were found in *o5-Ref* endosperm (Hunter et al., 2002). Several genes that could affect starch biosynthesis either directly or indirectly are included in the set of ~90 genes that were observed to have at least a twofold difference in mRNA level. Altered gene expression could result from signals derived from galacto- or phospholipid levels changed as a result of MGD1 deficiency and/or from altered metabolite levels.

Galactolipid Function in Embryo and Endosperm Development

Plastids are known to be crucial for various developmental processes, and nearly one-third of known *Arabidopsis* embryo-defective mutants affect plastid genes (Hsu et al., 2010; Inaba and Ito-Inaba, 2010). The phenotypes of *o5*⁻ plants bear striking parallels to maize *etched1* (*et1*) mutants. Like *o5*, weak *et1* alleles cause virescent seedlings that are initially pale but then become normal dark green (Sangeetha and Reddy, 1991; Scanlon et al., 1994; da Costa e Silva et al., 2004). Strong alleles cause defective endosperm development and embryo arrest, whereas heteroallelic combinations cause albino seedlings that die soon after germination. A striking aspect of *et1* endosperm defects is sectors of cells devoid of starch. Like *o5*, the primary defects of *et1* mutants appear to affect plastid function. The *et1* locus encodes a zinc ribbon protein that is targeted to plastids and appears to function in transcription (da Costa e Silva et al., 2004). Thus, functionally deficient plastids, impaired through distinct mechanisms, lead to highly similar plant and kernel phenotypes in *o5*⁻ and *et1*⁻ mutants.

Photosynthesis is thought to be critical for embryo development in many species, particularly dicots where embryos become green for much of seed development (Tschiersch et al., 2011). The physiological benefit of embryo photosynthesis is unclear, but one hypothesis is that the oxygen produced is critical to support respiration and maintain appropriate redox status in the hypoxic cellular environment of developing seeds. The ability to rescue *Arabidopsis mgd1-2* null mutant embryos with exogenous Suc would suggest that photosynthetic dysfunction is primarily responsible for the embryo lethality (Kobayashi et al., 2007). However, normal embryo development and seed germination in nonphotosynthetic albino mutants of *Arabidopsis* and maize (Prikryl et al., 2008; Liu et al., 2010) would suggest this explanation is not adequate. Furthermore, impaired photosynthesis seems an implausible explanation for the defects in *o5*⁻ maize endosperm development. Cereal grains have a single layer of photosynthetic collenchyma cells in the pericarp, but the endosperm does not contain chlorophyll (Tschiersch et al., 2011). As such, on segregating ears, the homozygous *o5-PS3038* mutant endosperms are surrounded by photosynthetically competent, genetically heterozygous maternal pericarp tissue, yet display defects. Therefore, a disruption of critical nonphotosynthetic plastid functions must be responsible for the mutant endosperm phenotype in maize.

As mentioned, assembly and function of several photosynthetic protein complexes require specific galactolipid interac-

tions (Liu et al., 2004; Sakurai et al., 2006; Hözl and Dörmann, 2007; Jones, 2007; Loll et al., 2007; Domonkos et al., 2008; Zhou et al., 2009). As such, it is likely that membrane composition could also affect plastid membrane protein complexes that function in processes other than photosynthesis. Plastids are centers for many metabolic processes, notably fatty acid biosynthesis (Joyard et al., 2010) and carotenoid biosynthesis (Lopez et al., 2008), which also involve integral membrane protein complexes. Several key hormones, including gibberellins (Yamaguchi, 2008), abscisic acid (Nambara and Marion-Poll, 2005), brassinosteroids (Boutté and Grebe, 2009), and cytokinins (Sakakibara, 2006), derive from plastidic isoprenoid metabolism. Perturbations in this system could readily explain the pleiotropic effects of *mgd1* mutations on development as well as the observed carotenoid deficiency. Other integral membrane protein complexes include the plastid protein import machinery (Kessler and Schnell, 2009). Thus, membrane composition could potentially affect multiple critical protein complexes involved in plastid processes that are required for cellular function and plant viability. The disruption of such other functions likely results in embryo lethality of mutants entirely lacking MGD1 such as *o5-PS3038*.

METHODS

Plant Materials

The mutations *o5-PS3038*, *o5-5288*, and *o5-313328* were isolated independently from self-pollinated ears of active *Mutator* lines in nontargeted mutagenesis experiments. The mutations were backcrossed into the B73 and/or W64A genetic backgrounds for at least three generations, and *o5-Ref* was backcrossed into the same inbreds for more than five generations. Nonviable mutations were maintained in the heterozygous state, and such plants were identified as backcross parents by appearance of ~25% opaque kernels on self-pollinated ears. Plants carrying *o5-Ref* were maintained in the homozygous state after backcrossing.

Kernels were collected from self-pollinated *o5-Ref/+* or *o5-PS3038/+* ears in the B73 genetic background segregating 25% homozygous mutant kernels. Controls were wild-type sibling kernels from the same segregating ears, with genotypes of either *o5/+* or *+/+*. Kernels from such ears were harvested at 15 or 20 DAP and used immediately for light microscopy analysis of endosperm and embryo tissue. The same tissues were used for comparison of *MGD1* transcript levels between wild-type and *o5-PS3038/o5-PS3038* mutant kernels. Mature kernels were used for TEM analysis.

Developing kernels used for analysis of enzymes, starch structures, transcript abundance, or polar lipid content were harvested from field-grown plants at 20 DAP, immediately frozen in liquid N₂, and stored at -80° until use. Where indicated, endosperm and embryo tissue was separated by dissection after thawing kernels on ice. Greenhouse-grown seedlings provided leaf, root, and shoot tissue for analysis of transcript levels and leaf tissue for polar lipid quantification.

Phylogenetic Analysis

Related sequences were identified in the NCBI protein database by performing a BLASTp search (Camacho et al., 2009). Selected sequences were aligned using ClustalW (Larkin et al., 2007), followed by manual editing, and the output alignment is shown in Supplemental Figure 1 online. Conserved residues in the output alignment file were shaded using the Boxshade program (http://www.ch.emblnet.org/software/BOX_form.html). The phylogenetic tree was produced with MEGA4 using

default parameters of the unweighted pair group method with arithmetic mean (UPGMA) algorithm, although neighbor joining gave an identical topology (Tamura et al., 2007). GenBank protein accessions used in the analysis are as follows: Zm MGD1 (the product of *o5*), NP_001142118; Os MGD1, Q69QJ7; At MGD1, NP_194906; Pp MGD1, XP_001758690; Pp MGD2, XP_001755870; Pt MGD, XP_002181685; Os MGD2, Q6UTZ2; Zm MGD3, NP_001170057; Zm MGD2, NP_001147778; Os MGD3, Q0DWQ1; At MGD3, NP_565352; and At MGD2, NP_568394.

RT-PCR

Plant tissues were frozen in liquid nitrogen and ground to a powder in a mortar and pestle. Total RNA was extracted with RNeasy plant mini kit (Qiagen). DNase-treated total RNA (3 μ g) was reverse transcribed in a 20- μ L reaction with Superscript III (Invitrogen) using oligo(dT) primers. Genomic DNA contamination was checked by PCR using ubiquitin primers on DNase-treated RNA as a template. The cDNA synthesis reaction (1 μ L) was used as template in PCR reactions with gene-specific primers. Ubiquitin primers or *ISA2* primers used in control reactions were previously described (Lee et al., 2009; Kubo et al., 2010). Primer sequences for amplification of *MGD1* mRNA were as follows: OP5-F, 5'-ATGCCACGAGACTGACCTCT-3'; OP5-R, 5'-TGAGGCTGAT-GGACTACACG-3'; *o5*-1, 5'-GATGGAAGAATGTATGGGTGCTTG-3'; *o5*-2, 5'-TGGGCCAA-ACCAGTCGGCAACT-3'; *o5*-3, 5'-GGAGTTCGGCGACGACTACCAG-3'; *o5*-4, 5'-GTGACAAGCTTATGGAACCATGTTGG-3'; *o5*-5, 5'-GAAGGTGCTGATCCTCATGA-3'; *o5*-6, 5'-GGAGTAAAACAATATCTACGATGAGT-TGC-3'; *o5*-7, 5'-GACCGAAGGATGAGCTCGAAGAG-3'. Primers for amplification of *MGD2* mRNA were as follows: MGD2-F, 5'-CATTCCACAGCACCTCGCCTA-3'; MGD2-R, 5'-CCACGACATATGGGACGTTCC-3'. Primers for amplification of *MGD3* mRNA were as follows: MGD3-F, 5'-CCTACTTGTACGCCAACGA-3'; MGD3-R, 5'-CCACGACATATGGG-ACGTTCC-3'.

PCR conditions using primers *o5*-1 to *o5*-7 were 94°C for 4 min, followed by 31 cycles of 94°C for 30 s, 55°C for 30 s, 72°C for 60 s, and a final extension of 72°C for 10 min. PCR conditions using primers OP5-F and OP5-R were 95°C for 2 min, followed by 30 cycles of 95°C for 30 s, 51°C for 30 s, 72°C for 60 s, and a final extension of 72°C for 5 min. Amplification of *MGD2* mRNA used the same protocol as for the OP5-F/OP5-R pair except that the annealing temperature was 60°C and 35 cycles were performed. *MGD3* mRNA was amplified using the same protocol as for the OP5-F/OP5-R pair except that the annealing temperature was 63°C. In all instances, the number of cycles was less than that necessary to reach a saturating level of signal observed as intensity of DNA bands after staining with ethidium bromide.

Lipid Analysis

Lipids were extracted from maize (*Zea mays*) seedling leaves or developing endosperm following the protocol specified by the Kansas Lipidomics Research Center for *Arabidopsis* leaf extractions (<http://www.k-state.edu/lipid/lipidomics/leaf-extraction.html>). The abundance of specific lipids in the extracts was determined by electrospray ionization-quadrupole tandem mass spectrometry according to lipid profiling protocols established by the facility (<http://www.k-state.edu/lipid/lipidomics/profiling.htm>). These methods detect phosphatidylcholine, lysophosphatidylcholine, phosphatidylserine, phosphatidylethanolamine, lysophosphatidylethanolamine, MGDG, DGDG, phosphatidylglycerol, phosphatidylinositol, and phosphatidic acid. Within each class defined by the head group, mass data specifically identify the total number of carbons and the total number of double bonds present in the two acyl groups combined.

Analyses of Carbohydrates and Starch Modifying Enzymes

Methods for determination of starch quantity in mature and developing endosperm tissue, starch extraction, determination of the linear chain

length distribution within amylopectin by fluorescence-assisted carbohydrate electrophoresis, and determination of amylose content by Sepharose CL-2B chromatography have been previously described (Kubo et al., 2010 and references therein). Detection of ISA enzyme activities and other starch modifying enzyme activities by zymogram analysis was performed as previously described (Kubo et al., 2010).

Microscopy

Specimens for visualization of embryo development were dissected from a self-pollinated *o5-PS3038/+* ear at 15 DAP. Kernels were fixed in formalin-acetic acid-alcohol and embedded in paraffin (Berlyn and Miksche, 1976). Microtome sections of 10- μ m thickness were affixed to glass microscope slides, deparaffinized in xylene, stained with Safranin O and fast green, and mounted in Permount. Leaf and endosperm specimens for histological analyses were fixed in 2% paraformaldehyde and 3% glutaraldehyde buffered in 0.1 M cacodylate, pH 7.2. For light microscopy analyses of endosperm, samples were embedded in LR White resin and sectioned to 1 μ m on a Leica EM UC6 ultramicrotome. Sections were stained with Periodic Acid Schiff's and methylene blue. For light microscopy analyses of leaf tissue, specimens were embedded in Spurr's resin, sectioned to 1 μ m, and stained with toluidine blue. Samples for TEM were also embedded in Spurr's resin and then postfixed with 1% osmium tetroxide, sectioned to 80 nm, affixed to grids, and stained with uranyl acetate and lead citrate. Histological specimens were photographed with an Olympus BX-60 microscope and a Jenoptik C-5 camera system. TEM examination was performed with a JEOL 2100 200 kV scanning and transmission electron microscope.

Accession Numbers

The GenBank/EMBL database accession number of the EST sequence used as a reference to identify the *o5* gene is EE189213. The reference for the cDNA sequence used to identify the position of specific mutations is accession number BT042676, and a cDNA sequence originally annotating the *o5* gene product is EU954700. The maize ubiquitin and *ISA2* mRNA sequences used as controls for RT-PCR analyses are specified by accession numbers EU959403 and AY172633, respectively.

Supplemental Data

The following materials are available in the online version of this article.

Supplemental Figure 1. Alignment of the Maize MGD Amino Acid Sequences with MGD Proteins from Other Species.

Supplemental Figure 2. Wild Type and Mutant Bundle Sheath Chloroplasts Visualized by TEM.

Supplemental Table 1. Allele and Phenotype Summary.

Supplemental Data Set 1. Lipid Profiling Raw Data.

Supplemental Data Set 2. Text File of Alignment of the MGD Amino Acid Sequences.

ACKNOWLEDGMENTS

We acknowledge the assistance of the Iowa State University William Keck Metabolomics Facility for analysis of starch chain length distributions and the Iowa State University Microscopy and Nanoimaging Facility for assistance with microscopy. Harry T. Horner provided helpful discussions interpreting TEM images. We also acknowledge the assistance of the Kansas Lipidomics Research Center, Kansas State University, for lipid analyses.

AUTHOR CONTRIBUTIONS

A.M.M., M.G.J., T.A.H.-B., and P.W.B. designed the research, performed research, analyzed the data, and wrote the article. Q.L. and G.Y. performed research. P.S.S. designed and performed the research.

Received May 9, 2011; revised May 9, 2011; accepted May 30, 2011; published June 17, 2011.

REFERENCES

- Andorf, C.M., Lawrence, C.J., Harper, L.C., Schaeffer, M.L., Campbell, D.A., and Sen, T.Z. (2010). The Locus Lookup tool at MaizeGDB: Identification of genomic regions in maize by integrating sequence information with physical and genetic maps. *Bioinformatics* **26**: 434–436.
- Awai, K., Maréchal, E., Block, M.A., Brun, D., Masuda, T., Shimada, H., Takamiya, K., Ohta, H., and Joyard, J. (2001). Two types of MGDG synthase genes, found widely in both 16:3 and 18:3 plants, differentially mediate galactolipid syntheses in photosynthetic and nonphotosynthetic tissues in *Arabidopsis thaliana*. *Proc. Natl. Acad. Sci. USA* **98**: 10960–10965.
- Badenhuizen, N.P. (1969). The Biogenesis of Starch Granules in Higher Plants. (New York: Appleton-Century-Crofts).
- Ball, S.G., and Morell, M.K. (2003). From bacterial glycogen to starch: Understanding the biogenesis of the plant starch granule. *Annu. Rev. Plant Biol.* **54**: 207–233.
- Barkan, A., and Martienssen, R.A. (1991). Inactivation of maize transposon Mu suppresses a mutant phenotype by activating an outward-reading promoter near the end of Mu1. *Proc. Natl. Acad. Sci. USA* **88**: 3502–3506.
- Barlow, P.W., and Sargent, J.A. (1978). The ultrastructure of the regenerating root cap of *Zea mays* L. *Ann. Bot. (Lond.)* **42**: 791–799.
- Benning, C. (2008). A role for lipid trafficking in chloroplast biogenesis. *Prog. Lipid Res.* **47**: 381–389.
- Benning, C., and Ohta, H. (2005). Three enzyme systems for galactoglycerolipid biosynthesis are coordinately regulated in plants. *J. Biol. Chem.* **280**: 2397–2400.
- Berlyn, G.P., and Miksche, J.P. (1976). *Botanical Microtechnique and Cytochemistry*. (Ames, IA: Iowa State University Press).
- Block, M.A., Dorne, A.J., Joyard, J., and Douce, R. (1983). Preparation and characterization of membrane fractions enriched in outer and inner envelope membranes from spinach chloroplasts. II. Biochemical characterization. *J. Biol. Chem.* **258**: 13281–13286.
- Botté, C., Jeanneau, C., Snajdrova, L., Bastien, O., Imberty, A., Breton, C., and Maréchal, E. (2005). Molecular modeling and site-directed mutagenesis of plant chloroplast monogalactosyldiacylglycerol synthase reveal critical residues for activity. *J. Biol. Chem.* **280**: 34691–34701.
- Boutté, Y., and Grebe, M. (2009). Cellular processes relying on sterol function in plants. *Curr. Opin. Plant Biol.* **12**: 705–713.
- Bruce, B.D. (1998). The role of lipids in plastid protein transport. *Plant Mol. Biol.* **38**: 223–246.
- Buléon, A., Colonna, P., Planchot, V., and Ball, S. (1998). Starch granules: Structure and biosynthesis. *Int. J. Biol. Macromol.* **23**: 85–112.
- Buttrose, M.S. (1960). Submicroscopic development and structure of starch granules in cereal endosperms. *J. Ultrastruct. Res.* **4**: 231–257.
- Camacho, C., Coulouris, G., Avagyan, V., Ma, N., Papadopoulos, J., Bealer, K., and Madden, T.L. (2009). BLAST+: Architecture and applications. *BMC Bioinformatics* **10**: 421.
- Cantarel, B.L., Coutinho, P.M., Rancurel, C., Bernard, T., Lombard, V., and Henrissat, B. (2009). The Carbohydrate-Active EnZymes database (CAZy): An expert resource for Glycogenomics. *Nucleic Acids Res.* **37**(Database issue): D233–D238.
- Coe, E.H., Jr., Neuffer, M.G., and Hoisington, D.A. (1988). The genetics of corn. In *Corn and Corn Improvement*, G.F. Sprague and J.W. Dudley, eds (Madison, WI: American Society of Agronomy; Crop Science Society of America; Soil Science Society of America), pp. 81–258.
- Cullis, P.R., and de Kruijff, B. (1979). Lipid polymorphism and the functional roles of lipids in biological membranes. *Biochim. Biophys. Acta* **559**: 399–420.
- da Costa e Silva, O., Lorbiecke, R., Garg, P., Müller, L., Wassmann, M., Lauert, P., Scanlon, M., Hsia, A.P., Schnable, P.S., Krupinska, K., and Wienand, U. (2004). The *Etched1* gene of *Zea mays* (L.) encodes a zinc ribbon protein that belongs to the transcriptionally active chromosome (TAC) of plastids and is similar to the transcription factor TFIS. *Plant J.* **38**: 923–939.
- Dinges, J.R., Colleoni, C., Myers, A.M., and James, M.G. (2001). Molecular structure of three mutations at the maize *sugary1* locus and their allele-specific phenotypic effects. *Plant Physiol.* **125**: 1406–1418.
- Domonkos, I., Laczkó-Dobos, H., and Gombos, Z. (2008). Lipid-assisted protein-protein interactions that support photosynthetic and other cellular activities. *Prog. Lipid Res.* **47**: 422–435.
- Dörmann, P., and Benning, C. (2002). Galactolipids rule in seed plants. *Trends Plant Sci.* **7**: 112–118.
- Dörmann, P., Hoffmann-Benning, S., Balbo, I., and Benning, C. (1995). Isolation and characterization of an *Arabidopsis* mutant deficient in the thylakoid lipid digalactosyl diacylglycerol. *Plant Cell* **7**: 1801–1810.
- Emanuelsson, O., Brunak, S., von Heijne, G., and Nielsen, H. (2007). Locating proteins in the cell using TargetP, SignalP and related tools. *Nat. Protoc.* **2**: 953–971.
- Finn, R.D., et al. (2010). The Pfam protein families database. *Nucleic Acids Res.* **38**(Database issue): D211–D222.
- Fishwick, M.J., and Wright, A.J. (1980). Isolation and characterization of amyloplast envelope membranes from *Solanum tuberosum*. *Phytochemistry* **19**: 55–59.
- Gounaris, K., Mannock, D.A., Sen, A., Brain, A.P.R., Williams, W.P., and Quinn, P.J. (1983). Polyunsaturated fatty acyl residues of galactolipids are involved in the control of bilayer/non-bilayer transitions in higher plant chloroplasts. *Biochim. Biophys. Acta* **732**: 229–242.
- Heinz, E. (1977). *Enzymatic reactions in galactolipid biosynthesis*. In *Lipids and Lipid Polymers in Higher Plants*, M. Tevini and H.K. Lichtenthaler, eds (Berlin, Heidelberg, and New York: Springer-Verlag), pp. 102–120.
- Holding, D.A., and Larkins, B.A. (2009). Zein storage proteins. In *Molecular Genetic Approaches to Maize Improvement*, A.L. Kriz and B.A. Larkins, eds (Berlin: Springer-Verlag), pp. 269–286.
- Holding, D.R., Otegui, M.S., Li, B., Meeley, R.B., Dam, T., Hunter, B.G., Jung, R., and Larkins, B.A. (2007). The maize *floury1* gene encodes a novel endoplasmic reticulum protein involved in zein protein body formation. *Plant Cell* **19**: 2569–2582.
- Hözl, G., and Dörmann, P. (2007). Structure and function of glycolipids in plants and bacteria. *Prog. Lipid Res.* **46**: 225–243.
- Hsu, S.C., Belmonte, M.F., Harada, J.J., and Inoue, K. (2010). Indispensable roles of plastids in *Arabidopsis thaliana* embryogenesis. *Curr. Genomics* **11**: 338–349.
- Hunter, B.G., Beatty, M.K., Singletary, G.W., Hamaker, B.R., Dilkes, B.P., Larkins, B.A., and Jung, R. (2002). Maize opaque endosperm mutations create extensive changes in patterns of gene expression. *Plant Cell* **14**: 2591–2612.

- Inaba, T., and Ito-Inaba, Y.** (2010). Versatile roles of plastids in plant growth and development. *Plant Cell Physiol.* **51**: 1847–1853.
- Jarvis, P., Dörmann, P., Peto, C.A., Lutes, J., Benning, C., and Chory, J.** (2000). Galactolipid deficiency and abnormal chloroplast development in the *Arabidopsis* MGD synthase 1 mutant. *Proc. Natl. Acad. Sci. USA* **97**: 8175–8179.
- Jones, M.R.** (2007). Lipids in photosynthetic reaction centres: Structural roles and functional holes. *Prog. Lipid Res.* **46**: 56–87.
- Jordan, P., Fromme, P., Witt, H.T., Klukas, O., Saenger, W., and Krauss, N.** (2001). Three-dimensional structure of cyanobacterial photosystem I at 2.5 Å resolution. *Nature* **411**: 909–917.
- Joyard, J., and Douce, R.** (1987). Galactolipid biosynthesis. In *The Biochemistry of Plants: Lipids: Structure and Function*, P.K. Stumpf, ed (New York: Academic Press), pp. 215–274.
- Joyard, J., Ferro, M., Masselon, C., Seigneurin-Berny, D., Salvi, D., Garin, J., and Rolland, N.** (2010). Chloroplast proteomics highlights the subcellular compartmentation of lipid metabolism. *Prog. Lipid Res.* **49**: 128–158.
- Kessler, F., and Schnell, D.** (2009). Chloroplast biogenesis: Diversity and regulation of the protein import apparatus. *Curr. Opin. Cell Biol.* **21**: 494–500.
- Kobayashi, K., Awai, K., Takamiya, K., and Ohta, H.** (2004). *Arabidopsis* type B monogalactosyldiacylglycerol synthase genes are expressed during pollen tube growth and induced by phosphate starvation. *Plant Physiol.* **134**: 640–648.
- Kobayashi, K., Kondo, M., Fukuda, H., Nishimura, M., and Ohta, H.** (2007). Galactolipid synthesis in chloroplast inner envelope is essential for proper thylakoid biogenesis, photosynthesis, and embryogenesis. *Proc. Natl. Acad. Sci. USA* **104**: 17216–17221.
- Kodrzycki, R., Boston, R.S., and Larkins, B.A.** (1989). The *opaque-2* mutation of maize differentially reduces zein gene transcription. *Plant Cell* **1**: 105–114.
- Kubo, A., Colleoni, C., Dinges, J.R., Lin, Q., Lappe, R.R., Rivenbark, J.G., Meyer, A.J., Ball, S.G., James, M.G., Hennen-Bierwagen, T.A., and Myers, A.M.** (2010). Functions of heteromeric and homomeric isoamylase-type starch-debranching enzymes in developing maize endosperm. *Plant Physiol.* **153**: 956–969.
- Lairson, L.L., Henrissat, B., Davies, G.J., and Withers, S.G.** (2008). Glycosyltransferases: Structures, functions, and mechanisms. *Annu. Rev. Biochem.* **77**: 521–555.
- Larkin, M.A., et al.** (2007). Clustal W and Clustal X version 2.0. *Bioinformatics* **23**: 2947–2948.
- Lee, A.G.** (2000). Membrane lipids: It's only a phase. *Curr. Biol.* **10**: R377–R380.
- Lee, B.H., Johnston, R., Yang, Y., Gallavotti, A., Kojima, M., Travençolo, B.A.N., Costa, Lda.F., Sakakibara, H., and Jackson, D.** (2009). Studies of *aberrant phyllotaxy1* mutants of maize indicate complex interactions between auxin and cytokinin signaling in the shoot apical meristem. *Plant Physiol.* **150**: 205–216.
- Liu, D., Gong, Q., Ma, Y., Li, P., Li, J., Yang, S., Yuan, L., Yu, Y., Pan, D., Xu, F., and Wang, N.N.** (2010). cpSecA, a thylakoid protein translocase subunit, is essential for photosynthetic development in *Arabidopsis*. *J. Exp. Bot.* **61**: 1655–1669.
- Liu, Z., Yan, H., Wang, K., Kuang, T., Zhang, J., Gui, L., An, X., and Chang, W.** (2004). Crystal structure of spinach major light-harvesting complex at 2.72 Å resolution. *Nature* **428**: 287–292.
- Loll, B., Kern, J., Saenger, W., Zouni, A., and Biesiadka, J.** (2007). Lipids in photosystem II: Interactions with protein and cofactors. *Biochim. Biophys. Acta* **1767**: 509–519.
- Lopez, A.B., Yang, Y., Thannhauser, T.W., and Li, L.** (2008). Phytoene desaturase is present in a large protein complex in the plastid membrane. *Physiol. Plant.* **133**: 190–198.
- Maréchal, E., Awai, K., Block, M.A., Brun, D., Masuda, T., Shimada, H., Takamiya, K., Ohta, H., and Joyard, J.** (2000). The multigenic family of monogalactosyl diacylglycerol synthases. *Biochem. Soc. Trans.* **28**: 732–738.
- Mongrand, S., Bessoule, J.-J., Cabantous, F., and Cassagne, C.** (1998). The C_{16:3}/C_{18:3} fatty acid balance in photosynthetic tissues from 468 plant species. *Phytochemistry* **49**: 1049–1064.
- Morell, M.K., Samuel, M.S., and O'Shea, M.G.** (1998). Analysis of starch structure using fluorophore-assisted carbohydrate electrophoresis. *Electrophoresis* **19**: 2603–2611.
- Myers, A.M., Morell, M.K., James, M.G., and Ball, S.G.** (2000). Recent progress toward understanding biosynthesis of the amylopectin crystal. *Plant Physiol.* **122**: 989–997.
- Nambara, E., and Marion-Poll, A.** (2005). Abscisic acid biosynthesis and catabolism. *Annu. Rev. Plant Biol.* **56**: 165–185.
- O'Shea, M.G., Samuel, M.S., Konik, C.M., and Morell, M.K.** (1998). Fluorophore-assisted carbohydrate electrophoresis (FACE) of oligosaccharides: efficiency of labelling and high-resolution separation. *Carbohydr. Res.* **307**: 1–12.
- Prikryl, J., Watkins, K.P., Friso, G., van Wijk, K.J., and Barkan, A.** (2008). A member of the Whirly family is a multifunctional RNA- and DNA-binding protein that is essential for chloroplast biogenesis. *Nucleic Acids Res.* **36**: 5152–5165.
- Sakakibara, H.** (2006). Cytokinins: Activity, biosynthesis, and translocation. *Annu. Rev. Plant Biol.* **57**: 431–449.
- Sakurai, I., Shen, J.-R., Leng, J., Ohashi, S., Kobayashi, M., and Wada, H.** (2006). Lipids in oxygen-evolving photosystem II complexes of cyanobacteria and higher plants. *J. Biochem.* **140**: 201–209.
- Salema, R., and Badenhuizen, N.P.** (1967). The production of reserve starch granules in the amyloplasts of *Pellionia daveauana* N. E. Br. *J. Ultrastruct. Res.* **20**: 383–399.
- Sangeetha, H.G., and Reddy, A.R.** (1991). Genetic and biochemical analysis of the *Etched (et)* mutant of *Zea mays* L. *Maydica* **36**: 343–354.
- Scanlon, M.J., James, M.G., Stinard, P.S., Myers, A.M., and Robertson, D.S.** (1994). Characterization of ten new mutations of the maize *Etched-1* locus. *Maydica* **39**: 301–308.
- Schmidt, R.J., Burr, F.A., Aukerman, M.J., and Burr, B.** (1990). Maize regulatory gene *opaque-2* encodes a protein with a “leucine-zipper” motif that binds to zein DNA. *Proc. Natl. Acad. Sci. USA* **87**: 46–50.
- Shannon, J.C., Garwood, D.L., and Boyer, C.D.** (2009). Genetics and physiology of starch development. In *Starch: Chemistry and Technology*, J.N. Bemiller and R.L. Whistler, eds (London: Academic Press), pp. 23–82.
- Shimajima, M., Ohta, H., Iwamatsu, A., Masuda, T., Shioi, Y., and Takamiya, K.** (1997). Cloning of the gene for monogalactosyldiacylglycerol synthase and its evolutionary origin. *Proc. Natl. Acad. Sci. USA* **94**: 333–337.
- Simidjiev, I., Stoylova, S., Amenitsch, H., Jávorfí, T., Mustárdy, L., Laggner, P., Holzenburg, A., and Garab, G.** (2000). Self-assembly of large, ordered lamellae from non-bilayer lipids and integral membrane proteins in vitro. *Proc. Natl. Acad. Sci. USA* **97**: 1473–1476.
- Tamura, K., Dudley, J., Nei, M., and Kumar, S.** (2007). MEGA4: Molecular Evolutionary Genetics Analysis (MEGA) software version 4.0. *Mol. Biol. Evol.* **24**: 1596–1599.
- Thompson, G., and Larkins, B.A.** (1994). Characterization of zein genes and their regulation in maize endosperms. In *The Maize Handbook*, M. Freeling and V. Walbot, eds (Berlin: Springer-Verlag), pp. 639–646.
- Tschiersch, H., Borisjuk, L., Rutten, T., and Rolletschek, H.** (2011). Gradients of seed photosynthesis and its role for oxygen balancing. *Biosystems* **103**: 302–308.
- Utsumi, Y., and Nakamura, Y.** (2006). Structural and enzymatic characterization of the isoamylase1 homo-oligomer and the isoamylase1-

- isoamylase2 hetero-oligomer from rice endosperm. *Planta* **225**: 75–87.
- Waters, M.T., and Langdale, J.A.** (2009). The making of a chloroplast. *EMBO J.* **28**: 2861–2873.
- Webb, M., and Green, B.** (1991). Biochemical and biophysical properties of thylakoid acyl lipids. *Biochim. Biophys. Acta* **1060**: 133–158.
- Welti, R., and Wang, X.** (2004). Lipid species profiling: a high-throughput approach to identify lipid compositional changes and determine the function of genes involved in lipid metabolism and signaling. *Curr. Opin. Plant Biol.* **7**: 337–344.
- Yamaguchi, S.** (2008). Gibberellin metabolism and its regulation. *Annu. Rev. Plant Biol.* **59**: 225–251.
- Yi, G., Luth, D., Goodman, T.D., Lawrence, C.J., and Becraft, P.W.** (2009). High-throughput linkage analysis of *Mutator* insertion sites in maize. *Plant J.* **58**: 883–892.
- Yun, M.-S., and Kawagoe, Y.** (2010). Septum formation in amyloplasts produces compound granules in the rice endosperm and is regulated by plastid division proteins. *Plant Cell Physiol.* **51**: 1469–1479.
- Zeeman, S.C., Smith, S.M., and Smith, A.M.** (2007). The diurnal metabolism of leaf starch. *Biochem. J.* **401**: 13–28.
- Zhou, F., Liu, S., Hu, Z., Kuang, T., Paulsen, H., and Yang, C.** (2009). Effect of monogalactosyldiacylglycerol on the interaction between photosystem II core complex and its antenna complexes in liposomes of thylakoid lipids. *Photosynth. Res.* **99**: 185–193.

Maize *opaque5* Encodes Monogalactosyldiacylglycerol Synthase and Specifically Affects Galactolipids Necessary for Amyloplast and Chloroplast Function

Alan M. Myers, Martha G. James, Qiaohui Lin, Gibum Yi, Philip S. Stinard, Tracie A. Hennen-Bierwagen and Philip W. Beecraft

Plant Cell 2011;23:2331-2347; originally published online June 17, 2011;

DOI 10.1105/tpc.111.087205

This information is current as of January 15, 2021

Supplemental Data	/content/suppl/2011/06/01/tpc.111.087205.DC1.html /content/suppl/2011/06/01/tpc.111.087205.DC2.html
References	This article cites 73 articles, 20 of which can be accessed free at: /content/23/6/2331.full.html#ref-list-1
Permissions	https://www.copyright.com/ccc/openurl.do?sid=pd_hw1532298X&issn=1532298X&WT.mc_id=pd_hw1532298X
eTOCs	Sign up for eTOCs at: http://www.plantcell.org/cgi/alerts/ctmain
CiteTrack Alerts	Sign up for CiteTrack Alerts at: http://www.plantcell.org/cgi/alerts/ctmain
Subscription Information	Subscription Information for <i>The Plant Cell</i> and <i>Plant Physiology</i> is available at: http://www.aspb.org/publications/subscriptions.cfm